

Olga B. Popovicheva^{1*}, Elena Volpert², Nikolay M. Sitnikov³, Marina A. Chichayeva⁴, Sara Padoan⁵

¹ SINP Moscow State University, Moscow, Russia

² Geographical Faculty, Moscow State University, Moscow, Russia

³ Central Aerological Observatory, Dolgoprudny, Moscow region, Russia

⁴ Peoples Friendship University of Russia (RUDN University), Moscow, Russia

⁵ Universität der Bundeswehr München, Neubiberg, Germany

*Corresponding author: polga@mics.msu.su

BLACK CARBON IN SPRING AEROSOLS OF MOSCOW URBAN BACKGROUND

ABSTRACT. Air quality in megacities is recognized as the most important environmental problem. Aerosol pollution by combustion emissions is remaining to be uncertain. Measurements of particulate black carbon (BC) were conducted at the urban background site of Meteorological Observatory (MO) MSU during the spring period of 2017 and 2018. BC mass concentrations ranged from 0.1 to 10 $\mu\text{g m}^{-3}$, on average 1.5 ± 1.3 and 1.1 ± 0.9 $\mu\text{g/m}^3$, in 2017 and 2018, respectively. Mean BC concentrations displayed significant diurnal variations with poorly prominent morning peak and minimum at day time. BC mass concentrations are higher at night time due the shallow boundary layer and intensive diesel traffic which results in trapping of pollutants. Wind speed and direction are found to be important meteorological factors affected BC concentrations. BC pollution rose identifies the North as the direction of the preferable pollution. A negative correlation between BC concentrations and wind speed confirms the pollution accumulation preferably in stable weather days. Relation of BC pollution to a number of agriculture fires is distinguishable by air mass transportation from South and South-Est of Russia and Western Europe. Mean season BC concentrations at rural and remote sites in different world locations are discussed.

KEY WORDS: air quality, black carbon, pollution, megacity

CITATION: Olga B. Popovicheva, Elena Volpert, Nikolay M. Sitnikov, Marina A. Chichayeva, Sara Padoan (2020) Black Carbon In Spring Aerosols Of Moscow Urban Background. *Geography, Environment, Sustainability*, Vol. 13, No 1, p. 233-143
DOI-10.24057/2071-9388-2019-90

INTRODUCTION

At present, air pollution by the smallest suspended particles (aerosols) is recognized as one of the most important environmental problems. Particulate matter characterized by a small aerodynamic diameter of less than 10 μm (PM10) contains environmentally hazardous components and it is recommended by the World Health Organization (WHO) as an air quality indicator. In accordance with the WHO air quality standards for PM10, a daily mean maximum permissible mass concentration of 50 $\mu\text{g/m}^3$ is established (WHO 2005). Black carbon (BC) is the light-absorbing component of aerosols, warming the atmosphere and thus affecting the Earth's radiation balance on a global scale (Bond et al. 2013). Estimates suggest that BC is the second most critical factor, following by carbon dioxide, contributing to global warming by direct forcing (Jacobson 2010). BC has drawn a considerable attention because of its environmental significance (Ramachandran and Rajesh 2007; Ahmed et al. 2014; Diapouli et al. 2017).

BC is mainly present in aerosols in urban environment (Mousavi et al. 2018), and thus it concerns local air quality and population health (Janssen et al. 2011). BC-containing particles are small enough to be readily inhaled into the human body and affects the respiratory system leading to exacerbate respiratory, cardiovascular, and allergic diseases, thus relating to adverse health effects (Pope III and Dockery 2006; Steiner et al. 2013). Epidemiological evidence links the exposure to BC with cardiopulmonary hospital admissions and mortality (WHO 2012).

Assessments of the ability for BC to affect the environment and health require a comprehensive study of the aerosol composition as well as a deep understanding of aerosol-related impacts. The comprehensive characterization of aerosols in the urban atmosphere makes it possible to identify sources of pollution and assess the consequences of effects of their emissions on air quality and human health. BC is increasingly recognized as the most important pollution contributor originating from anthropogenic activities, such as fossil fuel combustion (transport, energy production, residential heating) and biomass burning (domestic and wildfires). Diesel exhaust, which comprises high amounts of BC, is classified as a carcinogen for humans by the International Agency for Research on Cancer (IARC). Impact of traditional agriculture biomass burning (BB) activities on regional air quality is a major environmental concern, indicating that it may profoundly affect public health in urban areas (Popovicheva et al. 2017b).

BC emissions are found particularly large in most urbanized Asian cities where the rapid industrial and economic development has been accompanied by serious fine particle pollution of the atmosphere (Ohara et al. 2007; Chen et al. 2014). For US and European cities the source apportionment approach is intensively developed in order to estimate the most significant and dangerous combustion sources (Herich et al. 2011; Healy et al. 2017). An actual review on the status of ambient pollution in global megacities showed that the five most polluted megacities are Delhi, Cairo, Xi'an, Tianjin and Chengdu, all of which had an annual average concentration of PM2.5 greater than 89 $\mu\text{g/m}^3$ (Cheng et al. 2016). European

megacities (London, Moscow and Paris) had much lower annual average concentrations between 18 and 21 $\mu\text{g}/\text{m}^3$. However, these concentrations still are above the air quality guideline set by WHO to 10 $\mu\text{g}/\text{m}^3$ (WHO 2005).

Moscow megacity is the leader among all large cities of Russia on total number of inhabitants. However, for Moscow the situation is currently complicated by the existing lack of the aerosol composition and BC pollution assessments. High anthropogenic emissions of PM in Moscow can occur due to traffic, industry, heating, waste recycling, and construction. Additionally, secondary aerosol formation and long transportation can impact the particulate loading and composition, as it was occurred during an extreme smoke events related to intensive wildfires near the city (Popovicheva et al. 2014; Popovicheva et al. 2019).

However, Environmental Protection Agency "Mosecomonitoring" conducts the measurements for only PM10 and PM2.5 mass concentrations at some monitoring stations. The analysis of measured daily mean PM10 concentrations and calculated ones by chemical transport model CHIMERE showed the high temporal variability reflecting the influence of local sources and atmospheric processes (Kuznetsova et al. 2011; Gubanova et al. 2018). Presently, BC is not a subject of the consistent monitoring, it is remaining as a topic of a few scientific research performed in the Moscow center (Golitsyn et al. 2015; Kopeikin et al. 2018).

The purpose of this study is the analysis of the aerosol pollution related to BC in total PM10 mass in the urban background of the Moscow megacity. Spring season is chosen because this time is characterized by an elevated number of BC sources including the seasonal agriculture fires in surrounding areas and residential BB around the city. We measure and examine the diurnal variability of BC concentrations under real conditions of the diversity of urban sources of emissions and meteorological factors. Wind speed and direction affect BC concentrations while air mass transportation from fire-affected regions support the increased level of BC pollution in spring in the urban background.

MATERIALS AND METHODS

Measurement site

Moscow megacity covers an area of 2 561 km² and has a registered population exceeding 12.5 million in 2018. It is the largest city of Russia, and generally represents a typical urban area. Presently, in Moscow megacity 26 gaseous and particulate pollutants (PM10 and PM2.5) are under continuous measurements (Kul'bachevskii 2017). Around 630 industrial enterprises of various branches of mechanical engineering and metal working, power engineering, chemistry and petrochemistry, light and food industry, production of construction materials (including 30 000 stationary emissions sources) are registered. Around 50% of all pollutant emissions from industrial sources are emitted by enterprises producing and redistributing energy, gas, and water. Gaseous Automobile transport exhaust composes 95% of total city emissions. According the reports from the Moscow Committee of environmental protection and natural resources and the Department of the Federal State Statistics Service, industrial production zones occupy around 17% of the city area, from stationary sources fourteen biggest enterprises provide up to 85% of gross pollution (Bityukova and Saulskaya 2017) while transport emissions compose up to 93 % of gross pollution from mobile sources (Kul'bachevskii 2017). In total industrial emissions the processing productions, the production of oil products, and the production and power distribution of gas and water are dominated while gas composes 96.7% of fuel consumption. The biggest fractions of industrial emissions are NO_x (50%), CO (15%), SO₂ (16%) and 11% of volatile organic compounds. The Moscow city often faces serious traffic congestion problems because of the increased vehicle numbers; the total count of vehicles was registered as much as 4.6 million by the end of 2017 (Kul'bachevskii 2017). High speed of construction in Moscow additionally increases the aerosol loading in the atmosphere.

Black carbon mass concentration measurements were conducted at the rooftop of two-story building of the Meteorological Observatory of Moscow State University (MO MSU). MO is located at the territory of the MSU campus, southwest of the Moscow city (55°07'N, 37°52'E) (Fig. 1).

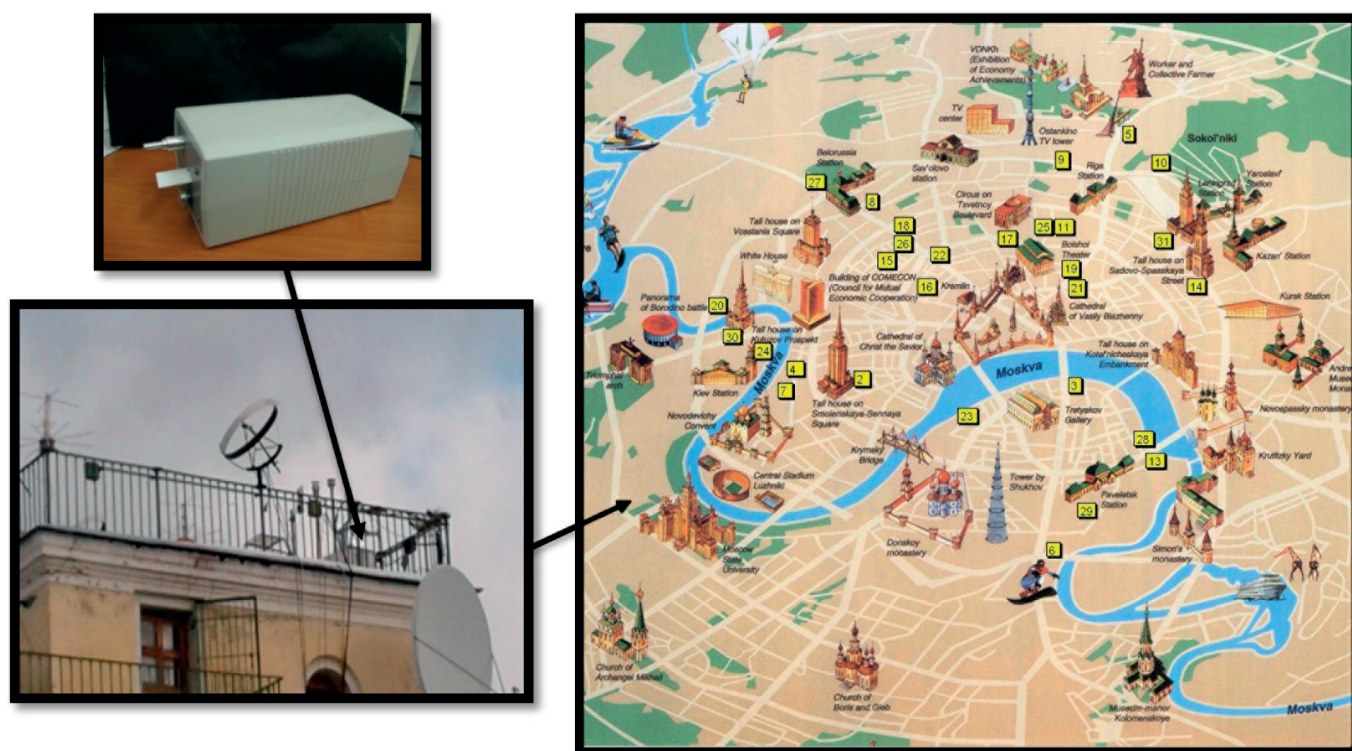


Fig. 1. Location of the portable aethalometer on the roof of Meteorological Observatory (MO) of MSU during spring campaigns of 2017 and 2018. MO MSU is on a Moscow city map

It takes place in an area of hills Vorobievy Gory which is well ventilated. There is no any industrial plants or commercial areas nearby (Fig. 2). At about 800 m to the north from the MO MSU there is the residential area and to the north-west the Lomonosovsky prospect highway is located. The closed industrial enterprises are central and quarter heating stations, and industrial areas which take place at the distance of 3 km and longer from the MSU. Therefore, MO MSU is considered operated as an urban background site.

Data collection

Aerosol equivalent BC concentrations (eBC) were measured using the portable aethalometer custom made by MSU/CAO. In this instrument the light attenuation caused by the particles depositing on a quartz fiber was analyzed at three wavelengths (450, 550, and 650 nm). eBC concentrations were determined by converting the time-resolved light attenuation to EBC mass at 650 nm and characterized by a specific mean mass attenuation coefficient as described elsewhere (Popovicheva et al. 2017a). Calibration parameter for quantification eBC mass was derived during parallel long-term measurements against an AE33 aethalometer (Magee Scientific) that operates at the same three wavelengths. Attenuation coefficient b_{atn} is defined as

$$b_{atn} = A \delta ATN / V \quad (1)$$

where A is the filter exposed area, V is the volume of air sampled, and δATN is the light attenuation defined as follows:

$$\delta ATN = \ln(I_0 / I) \quad (2)$$

where I_0 and I is the light intensity transmitted through unexposed and exposed parts of the filter, respectively. Good linear correlation between the aethalometer's attenuation coefficient b_{atn} and the eBC concentrations calculated with

the AE33 aethalometer (at 660 nm) was achieved ($R^2 = 0.92$). This allowed the estimation of eBC mass concentrations using the regression slope and intercept between b_{atn} at 650 nm and eBC of the AE33 aethalometer at 660 nm:

$$EBC = 3.3 \cdot 10^5 \cdot A \cdot \delta ATN / V \quad (3)$$

where 3.3×10^5 is the correction factor that includes the specific mass absorption coefficient for the MSU aethalometer calibrated against the AE33 aethalometer. Equation (3) assumes the mass absorption cross-section (MAC) adopted by AE33 equal to 9.89 m² g, values for A and V used to be in m² and m³. The constant MAC value adopted here is an approximation, assuming a uniform state of mixing for BC in atmospheric aerosol. This can be considered as a valid assumption in case of background aerosol measurements performed in this study. The level of uncertainty of eBC measurements was 30 ng/m³ for a 6 min integration time. Aethalometer filters were changed manually, when ATN approach the threshold value around 70 that corresponds the twice decreasing of light intensity transmitted.

Measurements were performed from 17 April to 25 May of 2017 and from 19 April to 23 May of 2018. Continuous measurements of meteorological parameters (temperature, relative humidity, pressure, precipitation, wind speed and wind direction) were performed each 3 hours routinely by MO MSU meteorological service. PM10 mass concentrations were collected by Mosecomonitoring using the tampered element oscillating microbalance TEOM 1400a (Thermo Environmental Instruments Inc., USA). These data were used for the comprehensive database of whole sampling runtime.

In spring time fires are usually observed on the South of the Moscow city, the agriculture practice with a purpose to remove the last year grass on the fields is widespread in this season. Biomass burning in residential areas around city is

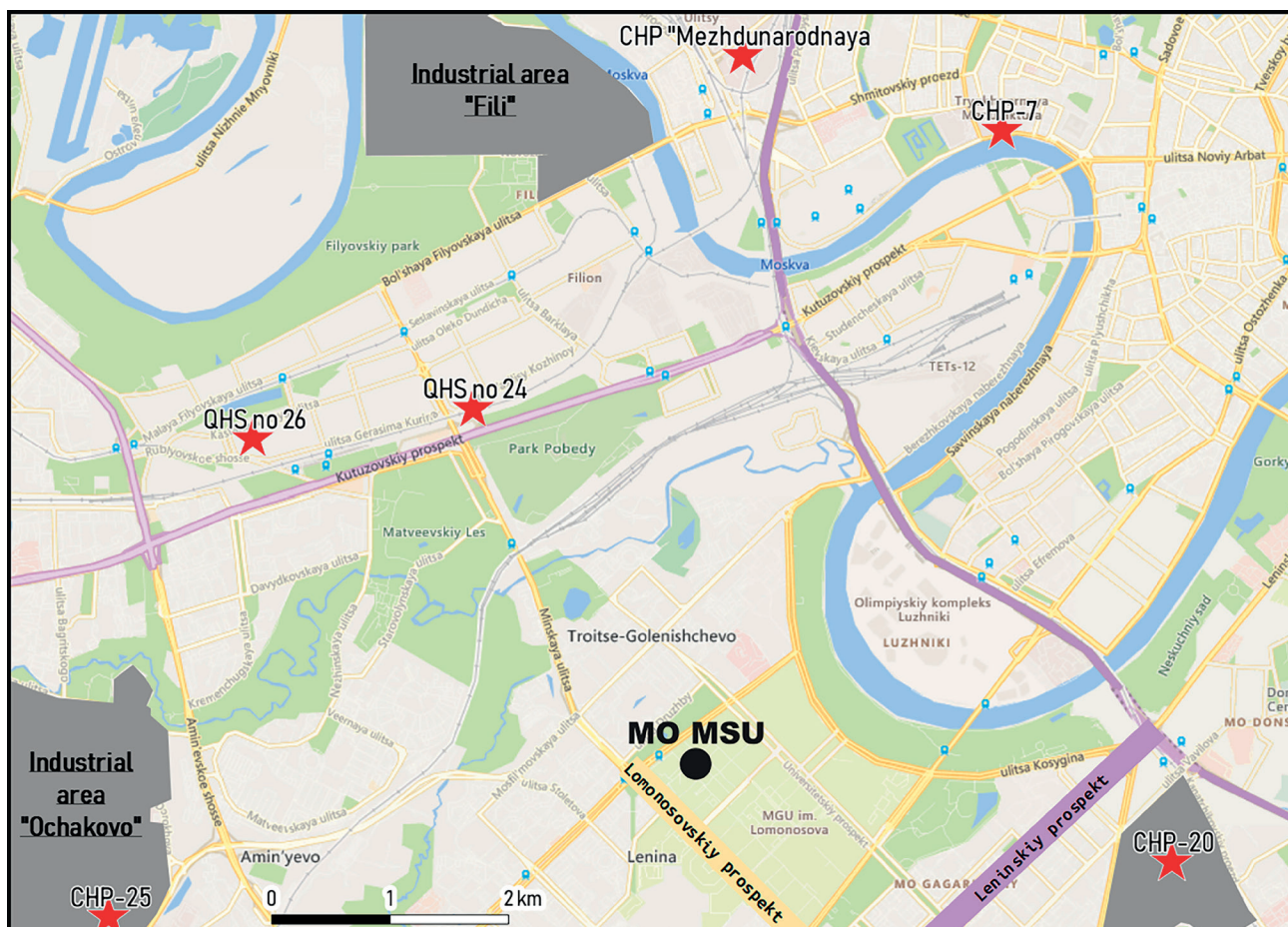


Fig. 2. The map of industrial areas and heating plans in Moscow around MSU. The black dot marked location of MO MSU. CHP – Central Heating Plan, DHS – District Heating Station

pronounced, especially during May holidays from 1 to 10 May. Therefore, air mass arriving to urban area due to long-range transportation may impact the air quality of the city, especially if direction of their transportation well correlates with fire-affected regions. To evaluate the air mass transportation impact the backward trajectories (BWT) were generated using NOAA HYbrid Single-Particle Lagrangian Integrated Trajectory (HYSPLIT) model of the Air Resources Laboratory (ARL) (Stein et al. 2015) with coordinate resolution equal to $1^\circ \times 1^\circ$ of latitude and longitude. The potential source areas were investigated using 2-day backward trajectories for air masses arriving each 12 hours to the MO MSU at 500 m heights above sea level (A.S.L.). Fire information was obtained from Resource Management System (FIRMS), operated by the NASA/GSFC Earth Science Data Information System (ESDIS). It is based on satellite observations which register the open flaming with temperature above 2000 K. Daily maps were related to the computed trajectories, providing a clear picture of the geographical location of fires, with the several kilometer resolutions. A number of fires which could affect air masses transported to the MO MSU was calculated as a sum of fires occurred at distance 0.5° on both latitude and longitude from BTW. The number of fires passed by BWT was estimated as the sum of the amounts of all points of fire caught on the back trajectories points or in their neighborhood of no further than 0.5° along the latitude and longitude. Number of fires indicates the BB-influenced days.

RESULTS AND DISCUSSION

Diurnal BC patterns

The diurnal eBC mass concentrations measured in spring seasons of 2017 and 2018 are shown in Figure 3. On a daily basis of 2017, there is an increase in concentrations starting

from 04:00, and the relatively prominent morning peak occurs at 7:00-09:00. eBC concentrations are found to be the smallest during midday until the evening, around 19:00. After this time the gradual increase of eBC is observed, reaching the maximum at 21:00-22:00. During 2018, the mean diurnal BC mass concentration is found to be constant from midnight to 04:00, the poorly noticeable peak occurs at around 05:00, and after the gradual decrease is marked until 20:00. Morning peak similar observed in spring of 2017 is not observed anymore in spring of 2018. The diurnal variation in mean BC mass concentrations is appeared around $1 \mu\text{g}/\text{m}^3$, approaching maximum 2 and 1.8 and minimum 0.9 and $0.5 \mu\text{g}/\text{m}^3$ during spring of 2017 and 2018, respectively.

The atmospheric abundance of BC is affected by both the stability of the boundary layer and anthropogenic activities in an urban environment (Ramachandran and Rajesh 2007). The nocturnal boundary layer depth is shallower than its daytime counterpart by a factor of 3–5. The development of a well-mixed layer height begins from 08:00, reaching maximum value around 14:00, decreases after 17:00, and later drops to the lowest level at night. The surface inversion after sunset results in the accumulation of BC, causing even higher concentrations in the late evening. It should be note that in many urban areas the evening peak is happened between 21:00 and 22:00 (Ramachandran and Rajesh 2007; Kozlov et al. 2011; Chen et al. 2014).

In large cites the BC morning peak is well observed for diurnal mass concentrations; it is attributed to the combined influence of the lower mixing layer height and vehicle traffic enhancement in the morning (Ramachandran and Rajesh 2007; Kozlov et al. 2011; Chen et al. 2014). The minimum BC concentrations are found during midday when there are fewer anthropogenic BC emissions, while the deeper boundary layer leads to a faster dispersion resulting in a dilution of BC concentrations at midday.

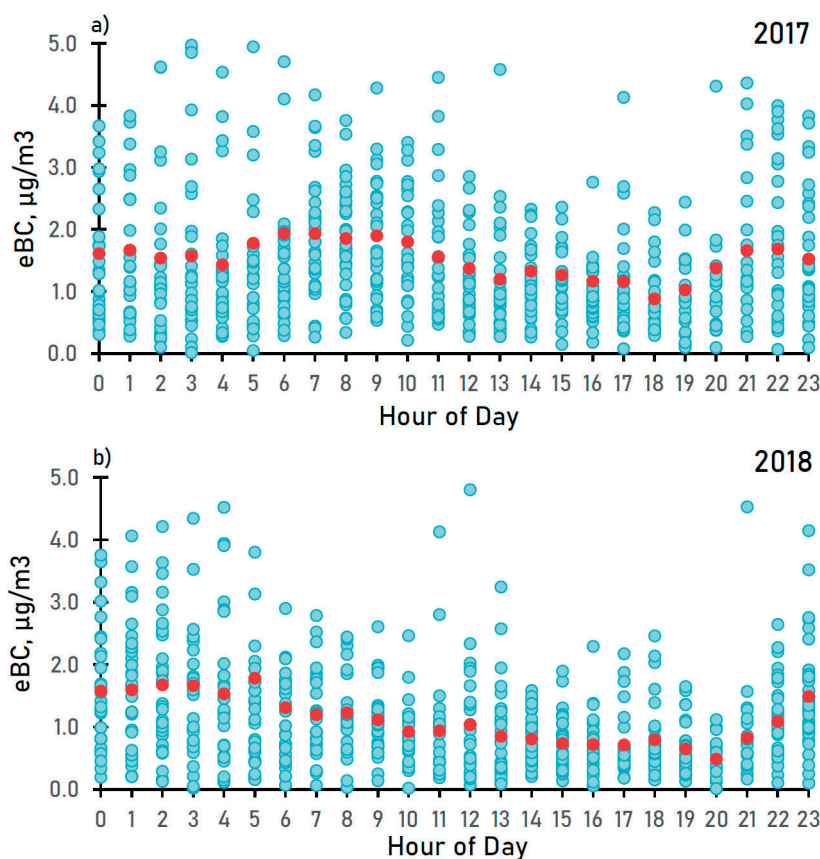


Fig. 3. Diurnal variations of hourly eBC concentrations during the sampling periods of a) 2017 and b) 2018 spring seasons. Plotted red points are the average values for aggregated data from the subsequent one hour on available days

Diesel and petrol are the major fossil fuels used for road transportation, the main part of the diesel vehicles are heavy-duty vehicles. Diesel vehicles are known to produce much more BC than the vehicles which run on gasoline (Weingartner et al. 1997). Heavy duty (e.g., trucks, buses etc.) diesel vehicle can contribute an average 42% BC to particulate matter (Reddy and Venkataraman 2002). Vehicles which run on leaded petrol and unleaded petrol (which do not have catalytic convertors) can give rise to 6 and 23% of BC in PM mass. They include two-wheelers such as scooters, motor bikes in addition to cars. In Moscow, a mixture of all vehicles runs on the roads and contributes to BC. In 2017 the Uniform interdepartmental information and statistical system (www.fedstat.ru) reported around 4640 000 vehicles, including 90.4 and 8.5 % of light and heavy duty cars and trucks, respectively, as well as 1,1 % of buses.

Stable high mean BC concentration from midnight to pre-dawn is observed especially prominent in 2018 (Fig. 3). Such diurnal profile is different from observed in large Russian city Tomsk (Kozlov et al. 2011) and Indian city Ahmedabad (Ramachandran and Rajesh 2007), and in megacity Athens (Diapouli et al. 2017). One reason may be related to increased emissions from diesel trucks (especially after 22:00) which could contribute to the higher BC concentration in the late evening (Garland et al. 2008). Here we should confirm that there is a restriction for heavy duty cargo vehicles to entry the Moscow city center during daytime, they are allowed to bring cargo only after midnight. Therefore, probably stable high BC observed later evening and during night time is due to the significant impact of diesel running vehicle emissions (almost from heavy duty cargo transport) in Moscow megacity.

Relationships between BC and meteorological parameters

The physical and chemical processes of BC emission, transformation, transportation, and accumulation in the atmosphere relate to meteorological conditions, i.e. wind speed and direction, transport of air masses, and the intensity of precipitation. The wind roses at MO MSU in both 2017

and 2018 spring seasons show the relatively homogeneous distribution of the wind direction during the sampling period, with the prevailing south-west direction and with a repeatability frequency up to 10% in this direction (Fig. 4). This finding confirms the observations of the South-West prevailing wind direction in the air layer from 40 to 500 m for the period of 2004–2014 at the MO MSU (Lokoshchenko 2015). The western component of the wind strengthens in spring and summer, that means that the South-Southwest direction is registered more rarely, and the West-Southwest one, more frequently.

The highest frequency of eBC pollution, around 13%, is found during northern wind, according to the eBC pollution roses (Fig. 5), when eBC mass concentrations approached 7 and 5 $\mu\text{g}/\text{m}^3$ in 2017 and 2018, respectively. Other directions of SW (225°), NW (315°), and NE (45°) relating to the high frequency of 6, 5, and 8%, respectively, indicate the most relevant emission source locations. Analysis of the geographical locations on a map shows that in the direction of SW (270–225°) the industrial area “Ochakovo” is located, and two quarter thermal stations take place in the direction of NNW and NW (around 335°), central heating plants can pollute MO MSU from north and NE (45°) (Fig. 2).

Wind speed is an important factor affecting BC concentrations: higher wind speeds contribute to stronger BC dispersion. It is probable that due to higher wind speeds BC produced from local sources are transported to other locations. Such phenomenon is typically observed in polluted urban area (Chen et al. 2014). It was found from BC measurements made in urban sites in Toronto that low wind speeds lead to much less dispersion of BC and the traffic emissions remain concentrated around the emission site (Sharma et al. 2002). It was also noted that as the traffic density was relatively constant through the measurement period, higher wind speeds have a dilution effect on BC. Correlation between wind speeds and BC mass concentrations may give an indication of the proximity of BC sources at the measurement site, while the absence of significant correlation shows that the BC originates from distant sources.

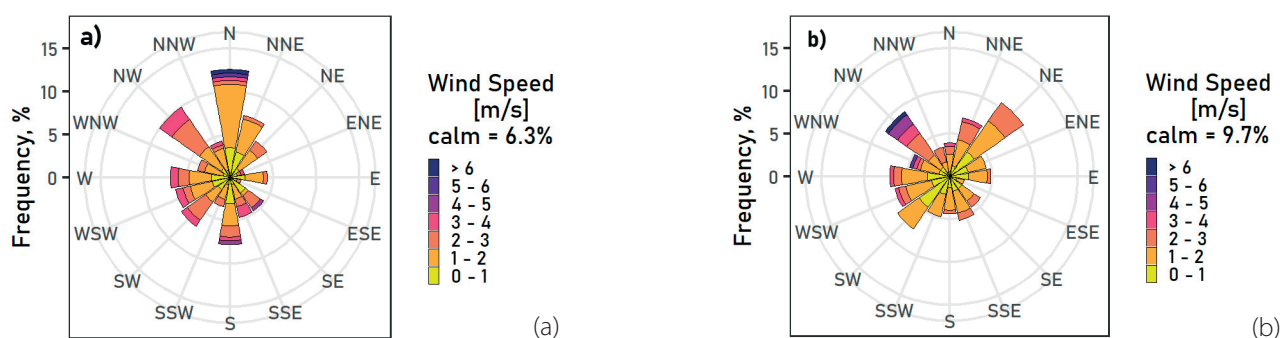


Fig. 4. Wind rose during spring season of a) 2017 and b) 2018

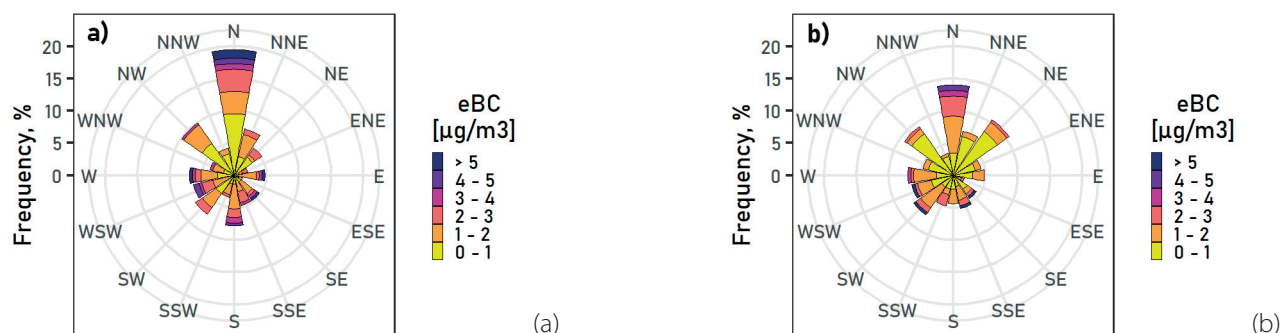


Fig. 5. eBC pollution rose during spring season of a) 2017 and b) 2018

A regression of BC mass concentrations with wind speed at MO MSU during spring seasons yield a negative regression coefficient (slope) -0.51 and -0.41 , respectively (Fig. 6). This indicates that with increase in wind speeds the BC mass concentrations would decrease, as seen. Such correlation between wind speeds and BC mass concentrations gives an indication of the intensive BC sources in a megacity.

Seasonal PM10 variations

The time series of PM10 mass concentrations over the whole period of observation is depicted in Fig. 7 and 8 for two-year spring seasons. In 2017, 1h mean PM10 concentrations showed a strong variation from lowest of $8 \mu\text{g}/\text{m}^3$ up to the highest value of $82 \mu\text{g}/\text{m}^3$, on average $22 \pm 16 \mu\text{g}/\text{m}^3$. In 2018, the PM10 variations from 2 to $90 \mu\text{g}/\text{m}^3$ were even more frequent but on short-term, on average $26 \pm 16 \mu\text{g}/\text{m}^3$. These values are comparable to PM10 concentrations averaged over warm season (May–September) obtained from the data for 236 urban background monitors in Europe in the periods of 2003–2006, on averaged amounts to $19.9 \mu\text{g}/\text{m}^3$ (Konovalov et al. 2009). For spring periods of 2014 and 2016 PM10 concentrations was 30.0 and $25.4 \mu\text{g}/\text{m}^3$, and 22.5 and $17.8 \mu\text{g}/\text{m}^3$ in the Moscow

center and at the suburban station, respectively; the difference of 26% between their average values is caused by an addition from urban sources (Kopeikin et al. 2018).

During spring seasons of our study PM10 concentrations exceeded the daily mean maximum permissible mass concentrations from one to seven times in 2017 and 2018, respectively. The longest episode of the highest PM10 was observed at MO MSU from 30 April until 3 May of 2017, on average $55 \pm 19 \mu\text{g}/\text{m}^3$. Almost at the same days, from 29 April until 2 May the ambient temperature has approached an abnormally high level for this season, $+ 21^\circ\text{C}$ (Fig. 9). In observation period of 2018, the permissible maximum PM10 values were exceeded seven times. the ambient temperature has approached $+ 21^\circ\text{C}$ twice, on 1 and 18 May.

Such exceeding of the air quality standards can occur during meteorological conditions unfavorable for pollutant dispersion, passage of cold atmospheric fronts, and arrival of air masses polluted by fires around the city (Kuznetsova et al. 2011). Analysis of location impact showed that the maximum PM10 concentration was observed at the stations in the eastern sector of the Moscow city and less often in the west of Moscow, at the MO MSU station (Kuznetsova et

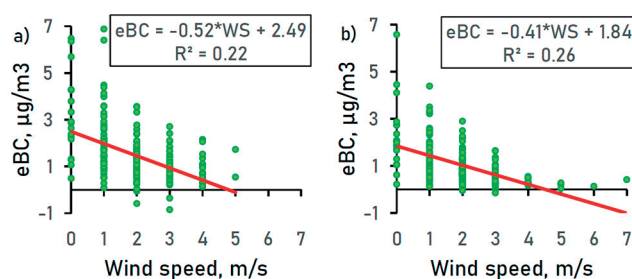


Fig. 6. Correlation of eBC mass concentration and wind speed (WS) during the sampling period of a) 2017, and b) 2018 spring seasons. Negative slope is obtained for linear fit of measurement points

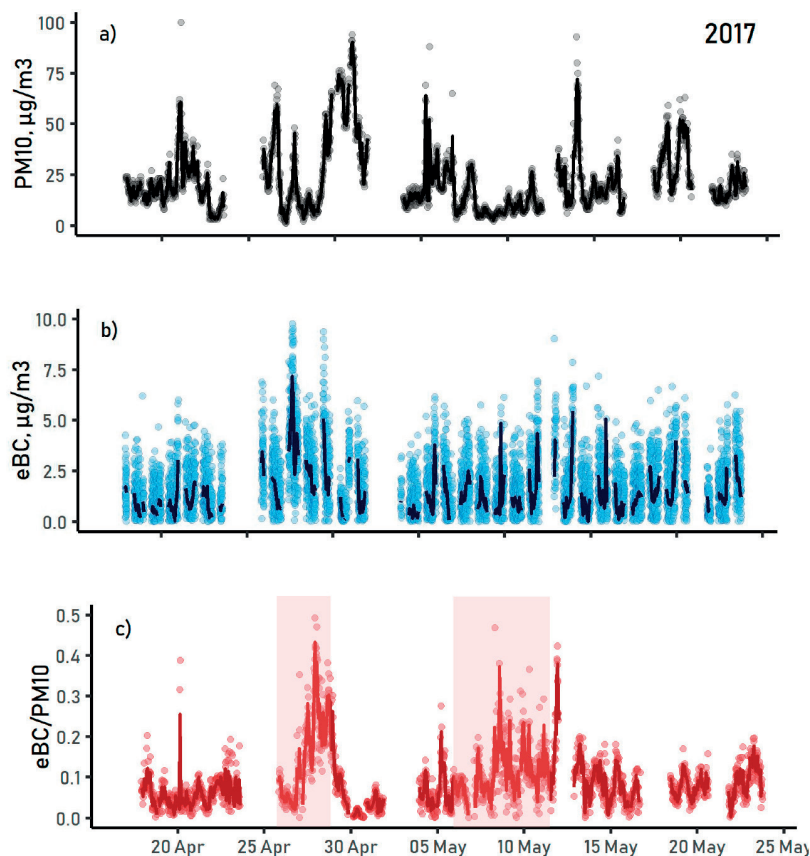


Fig. 7. 1-h mean (curve) and 1 min mean (dots) a) PM10 mass concentrations, b) eBC mass concentrations, and c) eBC/PM10 ratio in sampling period 2017 on the MO MSU. Pollution episodes are indicated.

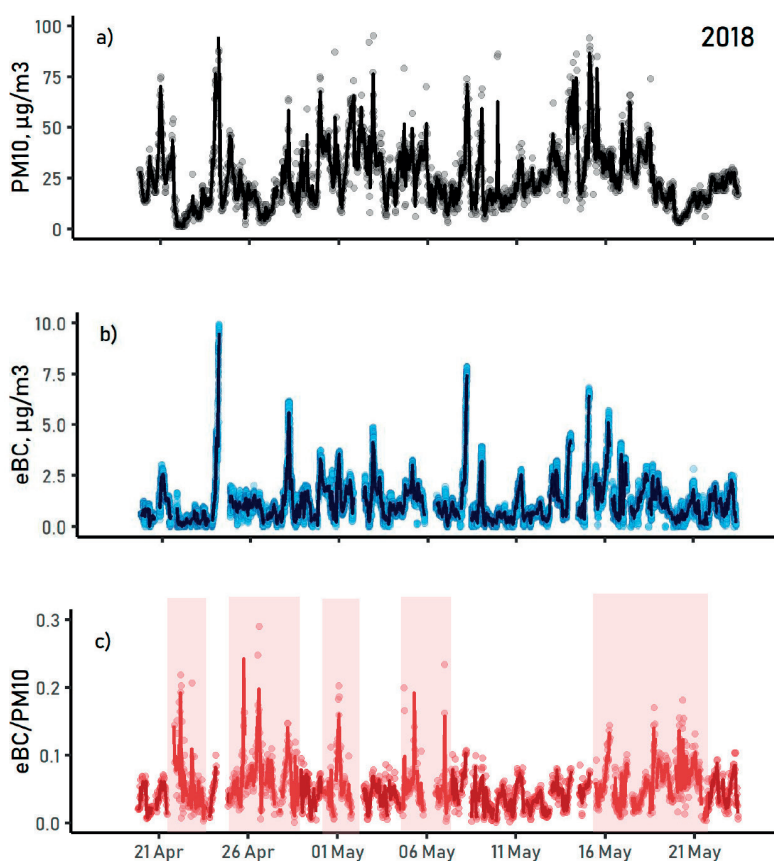


Fig. 8. 1-h mean (curve) and 1 min mean (dots) a) PM₁₀ mass concentrations, b) eBC mass concentrations, and c) eBC/PM₁₀ ratio in sampling period 2018 on the MO MSU. Pollution episodes are indicated.

al. 2011). This apparently reflects both local sources and a windward position in respect to the prevailing urban transfer. In the Moscow suburban station in Zelenograd city, both measured and calculated daily mean PM₁₀ concentration was almost always lower than at all urban stations, which confirms that a megalopolis is a significant source of aerosol emissions. Observation of PM₁₀ in summer showed a distinct correlation between short-term episodes of high PM₁₀ with the local temperature maximums (Kuznetsova et al. 2011).

A substantial positive correlation between temperature variations and PM₁₀ measurements at the European stations in the summer months was also established from the numerical analysis (Konovalov et al. 2009). The existence of this correlation can be attributed to the fact that, as a rule, high-temperature periods are followed by an anticyclonic (blocking) situations promoting the build-up of the atmospheric pollutants (Kuznetsova et al. 2011). The PM₁₀ concentration maximum is reached directly before or at the moment of the passage of cold front after the period of stagnation. A high PM₁₀ concentration can also be a result of the wind uplift of aerosols due to wind strengthening before the front passage in a warm sector of a cycle with sufficient precipitation and the air mass change, whereas the situation was preceded by dry weather favorable for the soil erosion.

In our study we observe relatively good correlation between high PM₁₀ and the local temperature maximums, with correlation coefficient R² equal 0.68 and 0.57 for 2017 and 2018, respectively (Fig. 10). It is expected that intensive precipitation may lead to strengthened wet aerosol deposition. Analysis of 24-h PM₁₀ variation with daily precipitation, shown on Fig. 10, indicates the decrease of PM₁₀ in relation with days of rain. The most prominently this phenomenon is observed for 18-20 May when during the period of the most intensive rains (more than 7.4 mm) we observed the lowest PM₁₀ mass (around 13 µg/m³).

Seasonal BC and level of pollution variations

The time series of 1-h mean eBC concentrations over the spring periods of sampling show the high eBC variability, ranged from 0.1 up to 5 and 10 µg/m³, on average 1.5 ± 1.3 and 1.1 ± 0.9 µg/m³, in 2017 and 2018, respectively (Fig. 7 and 8). Observations performed in the Moscow center showed the averaged BC concentrations of 4.4 and 1.7 µg/m³ while on suburban background station they were consistently less than 3.0 and 1.05 µg/m³, in spring 2014 and 2016 (Kopeikin et al. 2018).

Table 1 presents the mean BC concentrations obtained during the spring seasons at MO MSU, and rural and remote sites in different world locations. Comparisons show BC at MO MSU is lower than in European large cities like London (2.7 µg/m³) (Kendall et al. 2001) and Budapest (2.95 µg/m³) (Salma et al. 2004). However, the sites in these cities are classified as urban ones taking place in the city center. The closest to the measured BC value for MO MSU we find with the spring mean BC in the less polluted city in the Europe Helsinki, 1.03 µg/m³ (Järvi et al. 2008). The biggest BC was observed in the Indian and Chinese cities: around 5.5 and 8.8 µg/m³ in Dhanbad, the coal capital of India, and Guangzhou, the biggest megacity of South China (Singh et al. 2015) and (Wu et al. 2013), respectively.

Episodes of BC pollution can be identified by the increased ratio of eBC to PM₁₀ (eBC/PM₁₀). In 2017, the highest ratio more than 40% was observed from 27 April to 2 May, and around 9 and 13 May (Fig. 7). High temperature in the period of observations approaching a maximum at those days (Fig. 9) could relate to intensive biomass burning in the region around a city. Analyses of BWT arrived to the MO MSU during sampling period shows the highest number (48.9%) originating from North-West of the Moscow city. The remaining BWT arrived from North-East (28.1%), North - West (16.9%), and South - East (6.2%). Analyses of days of air mass transportation through fire areas demonstrates that the

Table 1. Mean season BC concentrations ($\mu\text{g}/\text{m}^3$) at rural and remote sites in different world locations

Site	Sampling period	BC	Reference
URBAN			
MO MSU, Moscow, Russia	April-May	1.1	this work
Helsinki, Finland	2017 – 2018	1.0	Jarvi et al. 2008
Budapest, Hungary	Spring 2004 – 2005	2.9	Salma et al. 2004
London 1, United Kingdom	April-May 2002	2.4	Kendall et al. 2001
Zurich, Switzerland	Spring 1996	1.2	Herich et al. 2011
La Reunion Island, France	Summer 2009 – 2010	0.5	Bhugwant and Brémaud 2001
Dhanbad, India	March-April 1998	5.5	Singh et al. 2015
Nanjing, China	March-April 2012	4.0	Wang et al. 2017
Mexico City, Mexico	April-May 2014	3.4	Salcedo et al. 2006
Guangzhou, China	April 2003	8.9	Wu et al. 2013
RURAL			
Yongxing Island, China	May-June 2008	0.5	Wu et al. 2013
Near Guangzhou, China	May-June 2008	2.6	Wu et al. 2013
Xilinhot, China	April 2005	2.0	Niu and Zhang 2010
Payerne, Switzerland	Summer 2008 – 2010	0.4	Herich et al. 2011

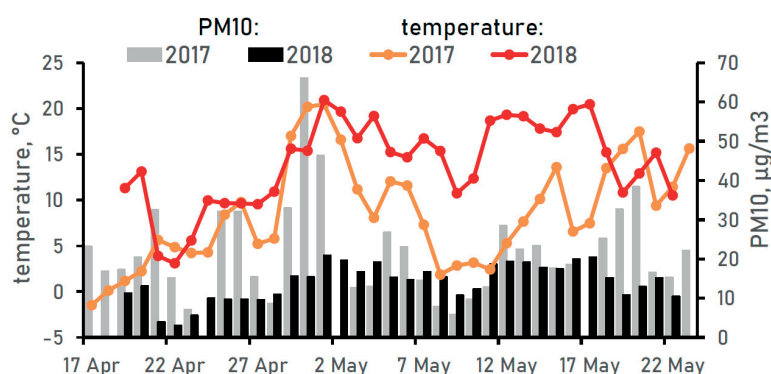


Fig. 9. 24-h mean temperature during the sampling period in 2017 (orange line) and 2018 (red line) and 24-h average PM10 mass concentrations in 2017 (gray) and 2018 (black)

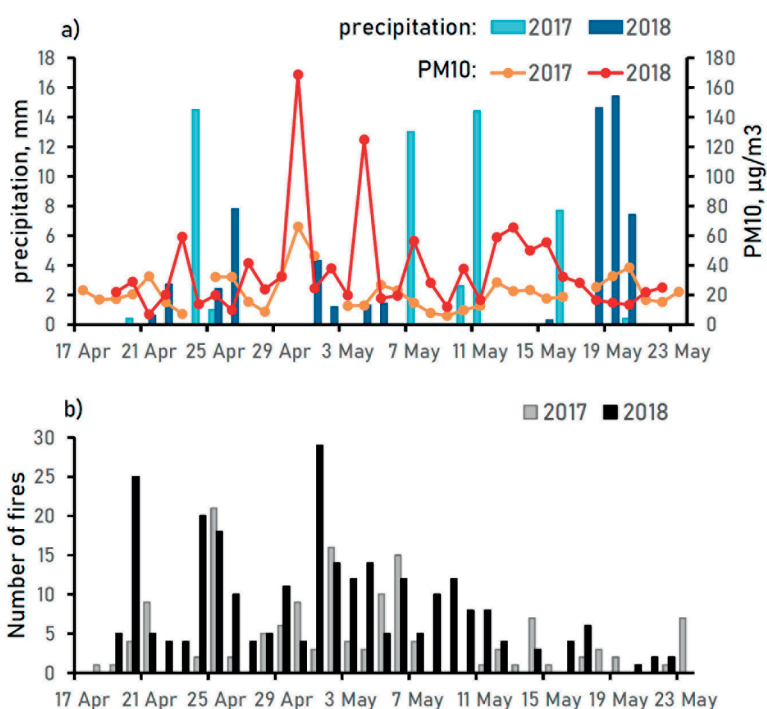


Fig. 10. a) Precipitation and 24-h average PM10 mass concentrations and b) number of fires during the spring seasons of 2017 and 2018

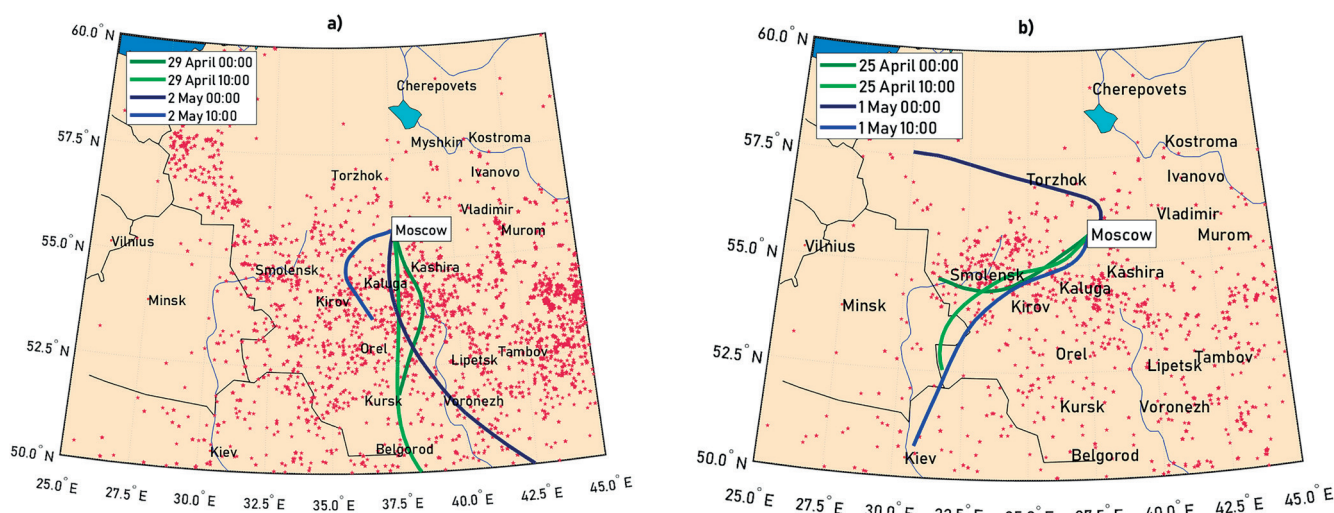


Fig. 11. 2-day backward air mass transportation from HYSPLIT model in the days of highest fires observed by FIRMS, 500 m a.s.l., a) 29 April and 2 May 2017, and b) 25 April and 1 May 2018. There are two trajectories for each day: one finished at 00:00 and second at 10:00 of the day.

biggest number of open flaming fires occurred on 26 April, 1–5 May (Fig. 10). Figure 11 shows the BWT arrived on 29 April and 2 May from areas with most intensive agriculture fires in south of Russia and Western Europe. Relation of abnormal temperature and the biggest number of open fires to the highest eBC/PM₁₀ at the days around 2 May confirms the reason of the BC pollution episode on urban background level. In the days of the biggest precipitations (07, 11, and 16 May) the low eBC/PM₁₀ ratios around 3–5 % were observed, relating to the washout effect.

In 2018, the level of pollution related to eBC/PM₁₀ showed the periodically repeated increased values of eBC/PM₁₀, up to 10 % (Fig. 8). Analyses of BWT arrived to the MO MSU during sampling period shows the highest number (34%) originating from north-east of the Moscow city. The remaining BWT arrived from South - West and North - West (25%), and South - East (16%). The biggest number of open flaming fires occurred in the South-East direction from the Moscow area at the days 20, 24–25 April, and 1 May (Fig. 10). Figure 11 shows the BWT arrived on 25 April and 1 May from areas of most intensive agriculture fires in South of Russia and Western Europe. Such observations confirm that high atmospheric pollutions in Moscow are mainly caused by the transport of pollutions from the regions with intense emissions over a distance of hundred kilometers (Golitsyn et al. 2015).

CONCLUSIONS

Measurements performed at the Meteorological Observatory MSU improve the luck of the analysis for the aerosol pollution related with BC as the most important

pollution contributor in total PM₁₀ mass in the urban background of Moscow megacity. The highest level of BC pollution, up to 40%, was observed in the days of the May holiday in Russia, related with abnormal high temperature and intensive agriculture fires in the south of Russia and biomass burning around the city. Diurnal profile in the spring season is observed to be different from other large cities: we note stable high BC at night, the less pronounced morning peak in comparison with nocturne BC concentrations, and significant increase of mean diurnal BC late in the evening. As Moscow is an urban, industrialized and densely populated city, the diurnal variations in BC mass concentrations can mainly be attributed to the vehicular emissions and transport from the surrounding regions. Mean spring BC concentrations at urban background of Moscow megacity are observed similar to one in European cities and significantly lower than in industrialized Asian cities, in well relations with intensive transport and using of gas, diesel, and gasoline instead of coal in Asia.

ACKNOWLEDGEMENTS

The authors thank the financial support from RSF project №18-17-00149 for BC measurement performance at MO MSU and air mass transportation modeling. Financial support from RSF project № 19-77-30004 for aethalometric methodic development and data analyses is acknowledged. ■

REFERENCES

- Ahmed T., Dutkiewicz V.A., Khan A.J. and Husain L. (2014). Long term trends in black carbon concentrations in the Northeastern United States. *Atmospheric Research*, 137, 49-57. doi: 10.1016/j.atmosres.2013.10.003
- Bhugwant C. and Brémaud P. (2001). Simultaneous measurements of black carbon, PM10, ozone and NOx variability at a locally polluted island in the Southern tropics. *Journal of Atmospheric Chemistry*, 39, 261-280. doi: 10.1023/A:1010692201459
- Bityukova V. and Saulskaya T. (2017). Changes of the anthropogenic impact of Moscow industrial zones during the recent decades. *Vestnik Moskovskogo Unversiteta, Seriya Geografiya*, 3, 24-33 (in Russian with English summary).
- Bond T.C., Doherty S.J., Fahey D.W., Forster P.M., et al.(2013). Bounding the role of black carbon in the climate system: A scientific assessment. *Journal of Geophysical Research: Atmospheres*, 118, 5380-5552. doi: 10.1002/jgrd.50171
- Chen X., Zhang Z., Engling G., Zhang R., et al. (2014). Characterization of fine particulate black carbon in Guangzhou, a megacity of South China. *Atmospheric Pollution Research*, 5, 361-370. doi: 10.5094/APR.2014.042
- Cheng Z., Luo L., Wang S., Wang Y., et al. (2016). Status and characteristics of ambient PM2.5 pollution in global megacities. *Environment International*, 89-90, 212-221. doi: 10.1016/j.envint.2016.02.003
- Diapouli E., Kalogridis A.-C., Markantonaki C., Vratolis S., et al.(2017). Annual variability of black carbon concentrations originating from biomass and fossil fuel combustion for the suburban aerosol in Athens, Greece. *Atmosphere*, 8, 34. doi: 10.3390/atmos8120234
- Dismuke C. and Egede L. (2015). The impact of cognitive, social and physical limitations on income in community dwelling adults with chronic medical and mental disorders. *Global Journal of Health Science*, 7(5), 183-195. doi: 10.5539/gjhs.v7n5p183
- Garland R., Yang H., Schmid O., Rose D., et al. (2008). Aerosol optical properties in a rural environment near the mega-city Guangzhou, China: implications for regional air pollution, radiative forcing and remote sensing. *Atmospheric Chemistry and Physics*, 8, 5161-5186. doi: 10.5194/acp-8-5161-2008
- Golitsyn G.S., Grechko E.I., Wang G., Wang P., et al. (2015). Studying the pollution of Moscow and Beijing atmospheres with carbon monoxide and aerosol. *Izvestiya Atmospheric and Oceanic Physics*, 51, 1-11. doi: 10.1134/S0001433815010041
- Gubanova D., Belikov I., Elansky N., Skorokhod A. and Chubarova N. (2018). Variations in PM2.5 surface concentration in Moscow according to observations at MSU Meteorological Observatory. *Atmospheric and Oceanic Optics*, 31, 290-299. doi: 10.1134/S1024856018030065
- Healy R., Sofowote U., Su Y., Debozs J., et al. (2017). Ambient measurements and source apportionment of fossil fuel and biomass burning black carbon in Ontario. *Atmospheric Environment*, 161, 34-47. doi: 10.1016/j.atmosenv.2017.04.034
- Herich H., Hueglin C. and Buchmann B. (2011). A 2.5 year's source apportionment study of black carbon from wood burning and fossil fuel combustion at urban and rural sites in Switzerland. *Atmospheric Measurement Techniques*, 4, pp. 1409-1420. doi: 10.5194/amt-4-1409-2011
- Jacobson M.Z. (2010). Short-term effects of controlling fossil-fuel soot, biofuel soot and gases, and methane on climate, arctic ice, and air pollution health. *Journal of Geophysical Research: Atmospheres*, 115. doi: 10.1029/2009JD013795
- Janssen N.A.H., Hoek G., Simic-Lawson M., Fischer P., et al. (2011). Black carbon as an additional indicator of the adverse health effects of airborne particles compared with PM10 and PM2.5. *Environmental Health Perspectives*, 119, 1691-1699. doi: 10.1289/ehp.1003369
- Järvi L., Junninen H., Karppinen A., Hillamo R., et al. (2008). Temporal variations in black carbon concentrations with different time scales in Helsinki during 1996–2005. *Atmospheric Chemistry and Physics*, 8, 1017-1027. doi: 10.5194/acp-8-1017-2008
- Kendall M., Hamilton R., Watt J. and Williams I. (2001). Characterisation of selected speciated organic compounds associated with particulate matter in London. *Atmospheric Environment*, 35, 2483-2495. doi: 10.1016/S1352-2310(00)00431-3
- Konovalov I., Beekmann M., Meleux F., Dutot A. and Foret G. (2009). Combining deterministic and statistical approaches for PM10 forecasting in Europe. *Atmospheric Environment*, 43, 6425-6434. doi: 10.1016/j.atmosenv.2009.06.039
- Kopeikin V., Emilenko A., Isakov A., Loskutova O. and Ponomareva T.Y. (2018). Variability of soot and fine aerosol in the Moscow region in 2014–2016. *Atmospheric and Oceanic Optics*, 31, 243-249. doi: 10.1134/S1024856018030089
- Kozlov V., Panchenko M. and Yausheva E. (2011). Diurnal variations of the submicron aerosol and black carbon in the near-ground layer. *Atmospheric and Oceanic Optics*, 24, 30-38. doi: 10.1134/S102485601101009X
- Kul'bachevskii A.O. (Ed.) (2017). Report on the state of the environment in Moscow in 2016. NIPI IGSP, Moscow. (in Russian).
- Kuznetsova I., Konovalov I., Glazkova A., Nakhaev M., et al. (2011). Observed and calculated variability of the particulate matter concentration in Moscow and in Zelenograd. *Russian Meteorology and Hydrology*, 36, 175-184. doi: 10.3103/S1068373911030046
- Lokoshchenko M. (2015). Wind direction in Moscow. *Russian Meteorology and Hydrology*, 40, 639-646. doi: 10.3103/S1068373915100015
- Mousavi A., Sowlat M.H., Hasheminassab S., Polidori A. and Sioutas C. (2018). Spatio-temporal trends and source apportionment of fossil fuel and biomass burning black carbon (BC) in the Los Angeles basin. *Science of the Total Environment*, 640, 1231-1240. doi: 10.1016/j.scitotenv.2018.06.022
- Niu S. and Zhang Q. (2010). Scattering and absorption coefficients of aerosols in a semi-arid area in China: Diurnal cycle, seasonal variability and dust events. *Asia-Pacific Journal of Atmospheric Sciences*, 46, 65-71. doi: 10.1007/s13143-010-0007-2
- Ohara T., Akimoto H., Kurokawa J.-I., Horii N., Yamaji K., Yan X. and Hayasaka T. (2007). An Asian emission inventory of anthropogenic emission sources for the period 1980–2020. *Atmospheric Chemistry and Physics*, 7, 4419-4444. doi: 10.5194/acp-7-4419-2007
- Pope III C.A. and Dockery D.W. (2006). Health effects of fine particulate air pollution: lines that connect. *Journal of the Air & Waste Management Association*, 56, 709-742. doi: 10.1080/10473289.2006.10464485
- Popovicheva O., Kistler M., Kireeva E., Persiantseva N., et al. (2014). Physicochemical characterization of smoke aerosol during large-scale wildfires: extreme event of August 2010 in Moscow. *Atmospheric Environment*, 96, 405-414. doi: 10.1016/j.atmosenv.2014.03.026
- Popovicheva O.B., Engling G., Ku I.-T., Timofeev M.A. and Shonija N.K. (2019). Aerosol emissions from long-lasting smoldering of boreal peatlands: chemical composition, markers, and microstructure. *Aerosol and Air Quality Research*, 19, 484-503. doi: 10.4209/aaqr.2018.08.0302
- Popovicheva O.B., Evangelidou N., Eleftheriadis K., Kalogridis A.C., et al. (2017a). Black carbon sources constrained by observations in the Russian high Arctic. *Environmental Science & Technology*, 51, 3871-3879. doi: 10.1021/acs.est.6b05832
- Popovicheva O.B., Shonija N.K., Persiantseva N., Timofeev M., et al. (2017b). Aerosol pollutants during agricultural biomass burning: A case study in Ba Vi region in Hanoi, Vietnam. *Aerosol and Air Quality Research*, 17, 2762-2779. doi: 10.4209/aaqr.2017.03.0111
- Ramachandran S. and Rajesh T. (2007). Black carbon aerosol mass concentrations over Ahmedabad, an urban location in Western India: comparison with urban sites in Asia, Europe, Canada, and the United States. *Journal of Geophysical Research: Atmospheres*, 112. doi: 10.1029/2006JD007488
- Reddy M.S. and Venkataraman C. (2002). Inventory of aerosol and sulphur dioxide emissions from India: I—fossil fuel combustion. *Atmospheric Environment*, 36, 677-697. doi: 10.1016/S1352-2310(01)00463-0

- Salcedo D., Onasch T.B., Dzepina K., Canagaratna M.R., et al. (2006). Characterization of ambient aerosols in Mexico City during the MCMA-2003 campaign with Aerosol Mass Spectrometry: results from the CENICA Supersite. *Atmospheric Chemistry and Physics*, 6(4), 925-946. doi: 10.5194/acp-6-925-2006
- Salma I., Chi X. and Maenhaut W. (2004). Elemental and organic carbon in urban canyon and background environments in Budapest, Hungary. *Atmospheric Environment*, 38, 27-36. doi: 10.1016/j.atmosenv.2003.09.047
- Sharma S., Brook J., Cachier H., Chow J., et al. (2002). Light absorption and thermal measurements of black carbon in different regions of Canada. *Journal of Geophysical Research: Atmospheres*, 107, AAC 11-1-AAC 11-11. doi: 10.1029/2002JD002496
- Singh S., Tiwari S., Gond D., Dumka U., et al. (2015). Intra-seasonal variability of black carbon aerosols over a coal field area at Dhanbad, India. *Atmospheric Research*, 161, 25-35. doi: 10.1016/j.atmosres.2015.03.015
- Stein A., Draxler R., Rolph G., Stunder B., et al. (2015). NOAA's Hysplit Atmospheric Transport and Dispersion Modeling System. *Bulletin of the American Meteorological Society*, 96, 2059-2077. doi: 10.1175/BAMS-D-14-00110.1
- Steiner S., Czerwinski J., Comte P., Popovicheva O., et al. (2013). Comparison of the toxicity of diesel exhaust produced by bio- and fossil diesel combustion in human lung cells in vitro. *Atmospheric Environment*, 81, 380-388. doi: 10.1016/j.atmosenv.2013.08.059
- Weingartner E., Keller C., Stahel W., Burtscher H. and Baltensperger U. (1997). Aerosol emission in a road tunnel. *Atmospheric Environment*, 31, 451-462. doi: 10.1016/S1352-2310(96)00193-8
- WHO (2005). WHO air quality guidelines for particulate matter, ozone, nitrogen dioxide and sulfur dioxide - Global Update 2005.
- WHO (2012). Health effects of black carbon. WHO.
- Wu D., Wu C., Liao B., Chen H., et al. (2013). Black carbon over the South China Sea and in various continental locations in South China. *Atmospheric Chemistry and Physics*, 13, 12257-12270. doi: 10.5194/acp-13-12257-2013

Received on July 13th, 2019

Accepted on November 7th, 2019